Nanoscale

PAPER

Published on 04 November 2026
Licensed under CC-BY 4.0

Check for updates

Cite this: DOI: 10.1039/d6nr03377f

Interfaces between cobalt phthalocyanines and $MoSe_2$: conditions for charge transfer and the nature of gap states

Carolin Schüle, †[a] Eric Juriatti,†[a] Peter Nagel,[b,c] Tim Parker,[a] Michael Merz,[b,c] Alfred J. Meixner,[a] Thomas Chassé,[a] Dai Zhang,[a] Stefan Schuppler,[b,c] Marcus Scheele *[a] and Heiko Peisert *[a]

Received 2nd September 2026,
Accepted 4th November 2026

DOI: 10.1039/d6nr03377f

rsc.li/nanoscale

The recently increasing research efforts devoted to layered transition metal dichalcogenides (TMDCs) derive from their novel electronic properties, which might be further tuned by the adsorption of molecules. However, the nature of interactions is often not fully understood, especially for comparably weakly interacting molecules, such as transition metal phthalocyanines (TMPcs). We studied interface properties between cobalt phthalocyanine (CoPc) or perfluorinated $CoPcF_{16}$ and molybdenum diselenide ($MoSe_2$) using photoelectron spectroscopy (PES), angle resolved photoelectron spectroscopy (ARPES), X-ray absorption spectroscopy (XAS) and photoluminescence spectroscopy. The interaction between $MoSe_2$ and cobalt phthalocyanines crucially depends on both the ionization potential of the molecule and the doping level of the substrate. Only for $CoPcF_{16}$ interfaces, a redistribution of electrons of the Co ion is observed, which can be associated with interfacial charge transfer. These effects are significantly more pronounced, if the $MoSe_2$ substrate is nominally n-doped. The results are discussed in the context of integer and fractional charge transfer, the latter associated with the formation of states within the band gap.

1. Introduction

Layered transition metal dichalcogenides (TMDCs), such as molybdenum disulfide and diselenide (MoS_2 and $MoSe_2$), as well as their alloys are currently the focus of interest due to their novel electronic properties including tunable band gaps in the optical or near infrared regime, large charge carrier mobilities and high exciton binding energies.[1–4] These aspects make the materials well-suited for application in optoelectronic devices such as photodetectors or field-effect transistors (FETs).[3,5] While many earlier studies focused on MoS_2, related TMDCs, including $MoSe_2$, appear to be even better suited for applications due to their physical properties such as conductivity or interlayer spacing.[6] Although $MoSe_2$ is a structural analogue of MoS_2, the ionization potential of $MoSe_2$ is up to 0.8 eV smaller and the band gap is reduced compared to MoS_2 (ref. 7, 8 and Fig. 1), which will affect also interface properties.

The adsorption of molecules results in TMDC/organic semiconductor hybrid interfaces which can lead to hybrid localized Frenkel- and delocalized Wannier-type excitons, enabling ultrafast interfacial charge transfer.[9] The choice of the TMDC/molecule combination affects crucially the interfacial electronic coupling and charge-transfer dynamics.[10,11] In the case of the adsorption of strong molecular electron acceptor molecules, such as 1,3,4,5,7,8-hexafluorotetracyanonaphthoquinodimethane (F_6TCNNQ), the difference in the ionization potentials can result in a (integer) charge transfer from the substrate to the LUMO of the molecule.[12] The interaction mechanism for weakly interacting, physiosorbed carbon molecules are still under investigation. Besides charge transfer, possible mechanisms also include dielectric screening and electronic hybridization at the interfaces under investigation.[13,14] It was demonstrated that optical properties can be distinctly affected by the adsorption of "weakly interacting" molecules (*e.g.* ref. 11 and 15–18). For example, a quenching of the low-temperature defect photoluminescence of MoS_2 was observed for heterostructures with transition metal phthalocyanines (TMPcs), depending strongly on the central metal atom of the phthalocyanine.[17] It is expected that these relatively overlooked molecular properties offer unique opportunities for tuning optical and electronic characteristics.[16] Recently, it was demonstrated

[a]*Institut für Physikalische und Theoretische Chemie, Universität Tübingen, 72076 Tübingen, Germany. E-mail: heiko.peisert@uni-tuebingen.de, marcus.scheele@uni-tuebingen.de; Fax: (+49)07071/29-5490; Tel: (+49)07071/29-76931*

[b]*Institute for Quantum Materials and Technologies (IQMT), Karlsruhe Institute of Technology (KIT), 76021 Karlsruhe, Germany*

[c]*Karlsruhe Nano and Micro Facility (KNMFi), Karlsruhe Institute of Technology, 76344 Eggenstein-Leopoldshafen, Germany*

† These authors contributed equally.

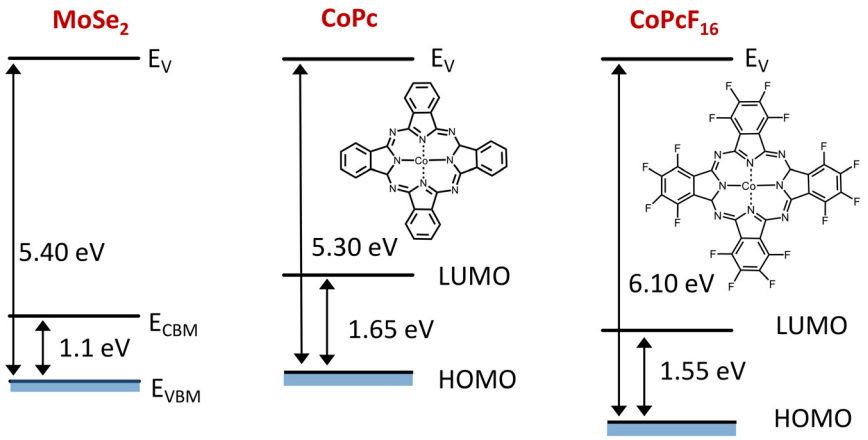


Fig. 1 Position of important energy levels of the $MoSe_2$ substrate and the molecules CoPc and $CoPcF_{16}$ with respect to the vacuum level E_v as obtained from ultraviolet photoemission spectroscopy (UPS). The CoPc or $CoPcF_{16}$ film thickness on $MoSe_2$ was >1.8 nm. The indirect band gap ($E_{VBM} - E_{CBM}$) for $MoSe_2$ and the optical gaps of the molecules (E(HOMO) − E(LUMO)) were taken from the literature (rounded to a half tenth of an eV).[26–28]

that the electrical characteristics of MoS_2 based FETs is distinctly affected by organic molecule adsorption.[5] Especially TMDC/TMPc heterostructures may exhibit novel electronic properties, which could be of high interest for efficient and flexible electronics, photonics and spintronics.[11,19–21]

Moreover, due to the chemical tunability of their electronic properties, TMPcs might be especially suited for systematic studies of the interfacial electronic structure. Generally, two different interaction paths are possible, *via* the central metal atom or the macrocycle. $CoPcF_X$ (X = 0, 16) often behaves differently, when compared to phthalocyanines with other transition metals, since the interaction might be governed by a local interaction between the Co $3d_{z^2}$ orbital and electronic states of the substrate.[22,23] The fluorination causes a distinct increase of the ionization potential by about 0.7–1.0 eV depending on the specific interface.[24–26] As a consequence, electronic interface properties like dipoles or charge transfer may change drastically.

Interfacial charge transfer can be described on a microscopic scale by integer charge transfer (ICT) or fractional charge transfer (FCT) models.[29–40] The mechanisms depend strongly on the strength of the interaction at the interface. Weakly interacting systems like physiosorbed molecules can be well described by the ICT model.[31–35] Within this model an integer interfacial charge transfer is expected if positive or negative charge transfer levels (ICT^+, ICT^-) are located above or below the work function of the substrate, respectively. In the case of a semiconductor as a substrate, the relative position to the valence band maximum (VBM) or conduction band minimum (CBM) becomes crucial if no charge carriers are present in the gap. Especially in the case of inequivalent adsorption sites, only some molecules can be integer charged, while others remain neutral.[30] The positive and negative integer charge transfer levels ICT^+ and ICT^- are associated with geometrically fully relaxed positive and negative polaron levels, often located 0.4–0.7 eV above the HOMO and below the LUMO (lowest unoccupied molecular orbital), respectively.[33] Fractional charge transfer is characterized by complex, bidirectional charge rearrangements accompanied with hybridization of orbitals at the interface.[29,30,36–39] For an interface between an inorganic semiconductor and a strong electron acceptor molecule, it was reported that both ICT and FCT can occur simultaneously, depending on the charge-carrier concentration (*i.e.* doping) of the inorganic semiconductor.[40]

In the present study, we investigate interfaces between CoPc or $CoPcF_{16}$ and $MoSe_2$ bulk crystals. The position of the energy levels of these materials with respect to the vacuum level E_v is compared in Fig. 1. Since the lowest unoccupied orbital (LUMO) is higher in energy than the valence band maximum (E_{VBM}) and the highest occupied molecular orbital (HOMO) is lower than the conduction band minimum (E_{CBM}) of $MoSe_2$, no integer charge transfer might be expected according to the integer charge transfer model.[31] However, we note that optical gaps were used for the determination of the E(HOMO) − E(LUMO) distance in Fig. 1, which solely consider the electronic relaxation and exhibit on the other hand an excitonic character (which lowers the energy gap). Therefore, especially for $CoPcF_{16}$, the fully relaxed ICT^- level might be close in energy to E_{CBM} of $MoSe_2$. In the present study we show that despite the relative positions of the important energy levels interfacial charge transfer can be observed and/or gap states can be formed, crucially depending on both the ionization potential of the molecule and the doping of $MoSe_2$.

2. Experimental section

$MoSe_2$ and nominally n-doped $MoSe_2$ (Re dopant, c = 10^{18}–10^{19} cm^{-3}) single crystals (2DSemiconductors Inc. (USA), grown by chemical vapor transport) were cleaved by adhesive tape in ultrahigh vacuum (UHV). The cleanliness and the azimuthal orientation of the surface were checked by X-ray photo-

 This journal is © The Royal Society of Chemistry 2026

electron spectroscopy (XPS) and angle resolved photoelectron spectroscopy (ARPES).

CoPc (Sigma Aldrich) and $CoPcF_{16}$ (BLD Pharmatech) were evaporated at rates of 0.05–0.2 nm min^{-1} and a temperature of 700–760 K from a home-built Knudsen cell. The evaporation rates were estimated from a quartz microbalance and the nominal film thicknesses was calculated from XPS intensity ratios using sensitivity factors from Yeh and Lindau[41] and the inelastic mean free path for organic molecules from Seah and Dench assuming layer-by-layer growth for each deposition step.[42] The monolayer thickness is assumed to be 0.35 nm, a typical intermolecular distance in phthalocyanine crystals.[43] In the case of layer-plus-island growth the average thickness might be somewhat higher than the nominal thickness.

Synchrotron based photoelectron spectroscopy (PES), angle resolved photoelectron spectroscopy (ARPES) and X-ray absorption spectroscopy (XAS) measurements have been performed at the WERA beamline at the KIT Light Source, Karlsruhe Research Accelerator (KARA, Karlsruhe, Germany). The base pressure was 2×10^{-10} mbar. For ARPES experiments the chosen photon energies were 135 eV (for the $MoSe_2$/CoPc interface) and 142.5 eV (for the (n-)$MoSe_2$/$CoPcF_{16}$ interfaces). The energy resolution for XAS was set to about 210 and 420 meV for the N K and Co L edge, respectively. For PES the energy resolution was 130 meV (ARPES), 200 meV ($h\nu$ = 550 eV), or better than 100 meV at other photon energies. The absorption was monitored indirectly by measuring the total electron yield (sample current). The X-ray absorption spectra have been normalized to the same step height well above the ionization threshold. For photon energy calibration the energy of the Ni-L_3 absorption edge of NiO at 853.0 eV was taken as a reference. For the evaluation of ARPES data we used the software ImageJ/Fiji.[44,45]

The PES measurements in the home lab (XPS and UPS) were performed using a multi-chamber UHV system (base pressure of 9×10^{-10} mbar) equipped with a Phoibos 150 Hemispherical Energy Analyzer (SPECS), an X-ray source with monochromator (XR 50 M, SPECS) and a UVS300 helium discharge lamp (SPECS). The energy resolution for XPS (excitation energy $h\nu$ = 1486.6 eV) and UPS ($h\nu$ = 21.22 eV), were 400 meV and 150 meV, respectively. The energy scale of PES was calibrated to reproduce the binding energies (BE) of Au $4f_{7/2}$ and Ag $3d_{5/2}$ (84.0 and 368.2 eV) and the Fermi level of the gold foil E_F = 0.0 eV.

The peak fitting of XPS spectra was performed using the program Unifit.[46] A Voigt profile peak shape (convolution of Gaussian and Lorentzian peaks) and a Shirley model background were used.

Luminescence measurements were performed on a home-built confocal optical microscope. The samples were excited with a 532 nm continuous wave laser (Nano-250, QIOPTIQ). The excitation beam was focused onto the sample using a parabolic mirror with a numerical aperture of 0.998, which also collected the emitted signal. The luminescence spectra were detected using a Teledyne Princeton Instruments HRS-500 spectrometer with a Teledyne Pixis 100 CCD camera using a 150 line per mm grating. All spectra were recorded with an excitation power of 150 μW in front of the parabolic mirror and an acquisition time of 30 s. For each sample a spectral map of 64 spectra was recorded using automatic positioning of the sample with an RHK Technologies SPM 100 controller. Optical images were recorded with a PerkinElmer SPCM-AQR-14 avalanche photodiode.

3. Results and discussion

3.1. Interfacial electronic structure from ARPES

ARPES is an ideal tool for the momentum-dependent analysis of the electronic structure at surfaces and interfaces. The formation of interface states with lower concentration can be monitored depending on the thickness of the deposited material.

In Fig. 2, band structures (ARPES M–Γ–K maps) of pristine $MoSe_2$ substrates and CoPc(F_{16}) covered $MoSe_2$ are shown. A more extended *k*-space range and the corresponding angle integrated 2D valence band spectra are depicted in Fig. S1 and S2 (SI). We note that the visible features in the band structure of $MoSe_2$ depend distinctly on $k_\perp$, which was considered in the selection of excitation energies (Fig. S3). Although G is already well visible for an excitation energy of 135.0 eV, we optimized the energy for the $CoPcF_{16}$ experiments further such that a sharp band is visible at the Gamma point, while bands originating predominantly from Mo and Se remain visible with adequate intensity (*cf.* Fig. S3). As an ancillary effect, cross sections change between 135.0 eV and 142.5 eV. According to Yeh and Lindau,[47] we can expect a decrease for C 2p of 17% and an increase for Mo 4d of about 5%. Also, the thickness is not exactly the same for each experiment, but always in the monolayer range. Together with lower thickness compared to the other experiments, this may explain the weaker molecule related features for CoPc/$MoSe_2$ (Fig. 2a/d).

As visible in Fig. 2, the initial position of the Fermi level for the nominally undoped substrates deviates distinctly from the mid-gap position (Fig. 2a and b) considering the indirect band gap of 1.10 eV for bulk $MoSe_2$.[27,28,48] Also, the maximum of the Γ point of the pristine substrates is not exactly at the same position when comparing the two pristine cleaves in Fig. 2a and b. We may ascribe this behavior to step edges and/or non-detectable traces of adsorbates which could already induce n-doping of the substrate. For the doped $MoSe_2$ (Fig. 2c), the position of the Γ point is in agreement to n-doping, but we can assume that the carrier concentration is significantly higher compared to the nominally undoped substrates. Even occupied states close to the Fermi level can be detected (see inset of Fig. 2c).

After deposition of CoPc (Fig. 2d), additional non-dispersive features can be detected. The origin of these features can be ascribed to the molecule, intensity close to the Γ point arises from the highest molecular orbital (HOMO). For CoPc and $CoPcF_{16}$, the HOMO is essentially formed from orbitals of the macrocycle while features arising from the Co central atom

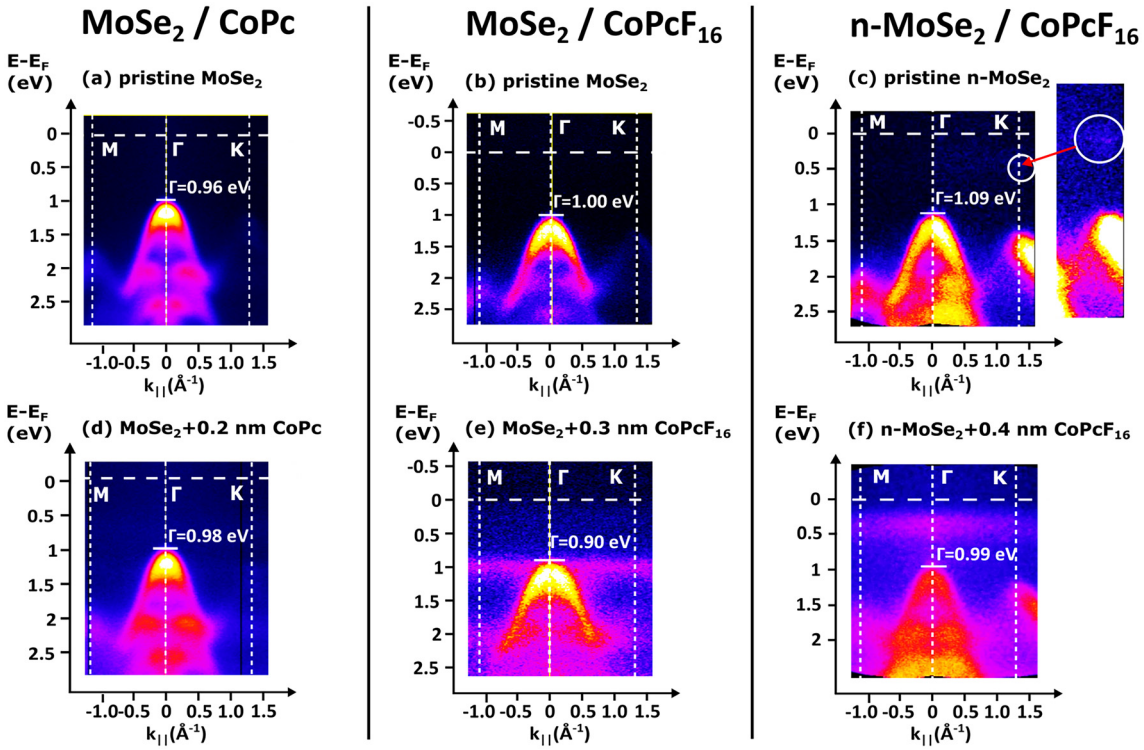


Fig. 2 Comparison of ARPES band structures before and after deposition of CoPc or $CoPcF_{16}$: (a–c) pristine substrates, (d–f) coverages in the monolayer range. The same crystal was used for (a) and (b), the slight energy shift is ascribed to inhomogeneities of the crystal. For the nominally n-doped crystal (c), intensity at the doping level can be seen in vicinity to the K point.

appear at about 0.85 eV higher binding energy (see, *e.g.* ref. 23 and 49). Also, for $CoPcF_{16}$ on $MoSe_2$ (Fig. 2e), the non-dispersive HOMO close to Γ is clearly visible. Most importantly, additional intensity within the gap of $MoSe_2$ is detectable, which can be interpreted as molecule-induced gap states. The formation of additional states in the gap is even more evident for $CoPcF_{16}$ on n-$MoSe_2$ (Fig. 2f), where a non-dispersive line is clearly visible at a distance <0.5 eV to the Fermi level.

The possible formation of gap states can be also traced in the integrated 2D valence band spectra (Fig. S2). The HOMO-onset for monolayer coverages is hardly visible due to the superposition with the valence band maximum of $MoSe_2$ in all three cases. Only for the $MoSe_2$/$CoPcF_{16}$ interfaces (Fig. S2b and c) interface states are clearly visible, more pronounced for n-$MoSe_2$/$CoPcF_{16}$ interface (Fig. S2c), indicating a strong interfacial interaction.

3.2. Involvement of the Co atom of the TMPcs in the interface interaction

An interaction *via* the central cobalt atom of phthalocyanines can be detected by the analysis of Co L edge XAS spectra or Co 2p XPS spectra as a function of film thickness. Especially Co L edge XAS spectra are very sensitive to the electronic structure of the Co atom. The shape of the spectra is determined to a large extent by multiplet effects; the reason is the strong overlap of the core wave function with the valence wave functions.[50] Depending on the orientation of the electric field vector of the incoming synchrotron light/beam and the orientation of the molecules, transitions into orbitals with mostly out-of-plane (d_{xz}, d_{yz}, and d_{z^2}) or mostly in-plane components ($d_{x^2-y^2}$ and d_{xy}) are possible, which explains their strong angular dependency (*e.g.* ref. 23). For flat lying, planar TMPcs with D_{4h} symmetry and p-polarized synchrotron radiation, we probe transitions at normal incidence (θ = 90°) into orbitals lying in the molecular plane and at grazing incidence (θ = 20°) preferentially into orbitals with out-of-plane character. In the case of CoPc, due to multiplet effects we expect 16 possible $2p^63d^7 \rightarrow 2p^53d^8$ transitions.[50] The orbital with the highest energy is $d_{x^2-y^2}$ (b_{1g}); transitions into this orbital exhibit in-plane character. The third hole in the ground state is expected in the d_{z^2} (a_{1g}), an orbital with distinct out-of-plane character; likely also mixed valences have to be considered.[23,51,52]

From the angular dependence of both Co L and N K spectra of thicker films with a shape typical for bulk-like films where influences of the substrate are almost negligible (*cf.* ref. 23), we conclude that CoPc and $CoPcF_{16}$ are oriented preferentially flat-lying on $MoSe_2$ bulk substrates (SI, Fig. S4). Unfortunately, N K spectra for monolayer coverages are dominated by the substrate related absorption at the Mo M edge, which makes a detailed analysis difficult.

In Fig. 3, we show angle dependent Co $L_{2,3}$ edge XAS spectra for CoPc or $CoPcF_{16}$ coverages in the monolayer range on (n-) $MoSe_2$. The L_3 edge transitions between 770 and 785 eV that are polarized perpendicular to the molecular plane are

 This journal is © The Royal Society of Chemistry 2026

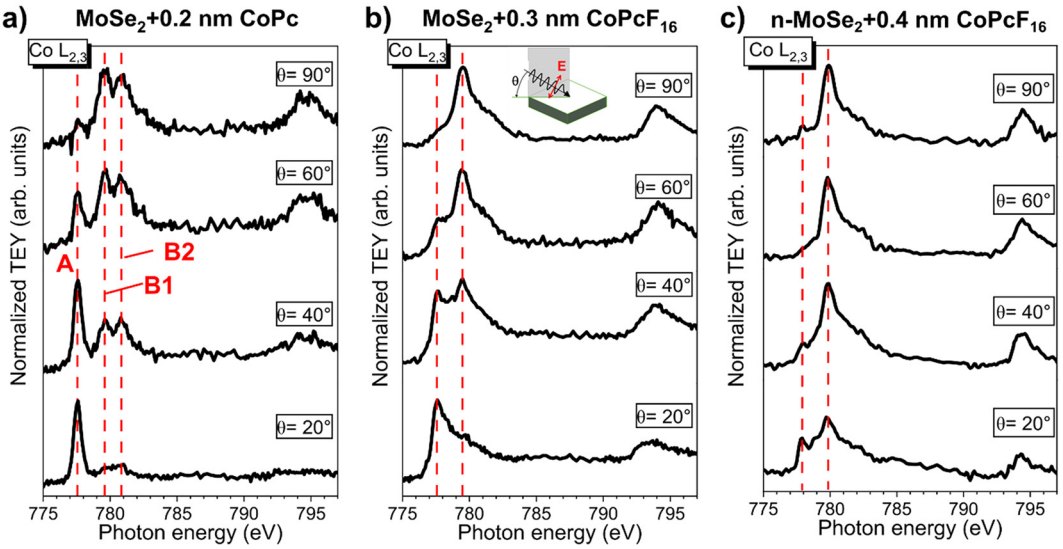


Fig. 3 Angle dependent Co $L_{2,3}$ edge XAS spectra for coverages in the monolayer range (a) CoPc/$MoSe_2$, (b) $CoPcF_{16}$/$MoSe_2$, (c) $CoPcF_{16}$/n-type $MoSe_2$. Only for CoPc/$MoSe_2$ the spectral shape is very similar to the bulk indicating the absence of charge transfer across the interface involving the Co atom of CoPc.

denoted "A", and features that are polarized within the molecular plane are denoted "B" (Fig. 3a). The measurement geometry is shown as an inset in Fig. 3b. The shape and the angular dependence for CoPc on $MoSe_2$ is in very good agreement to preferentially flat lying molecules in bulk-like films (*e.g.* ref. 23), indicating the absence of interactions involving the Co atom of CoPc at the $MoSe_2$ interface. In contrast, the shape of the XAS spectra for $CoPcF_{16}$ on (n-)$MoSe_2$ (Fig. 3b and c) is distinctly different. First, the relative intensity of A at about 777.5 eV is clearly suppressed at grazing incidence, an observation which seems to be even more pronounced for $CoPcF_{16}$ on n-$MoSe_2$ (Fig. 3c). Second, feature B2 (780.8 eV) almost disappeared, only B1 (779.6 eV) remains. Such behaviour was observed for cobalt phthalocyanines on other substrates (*e.g.* ref. 23), indicating a redistribution of the d-electrons at the central metal atom of the phthalocyanine at the interface to $MoSe_2$, which might be accompanied with interfacial charge transfer.

The XAS results are supported by complementary XPS measurements in the home lab. In Fig. 4, we show Co $2p_{3/2}$ core level spectra for the three interfaces as a function of the film thickness ranging from (sub-)monolayer to several multi-

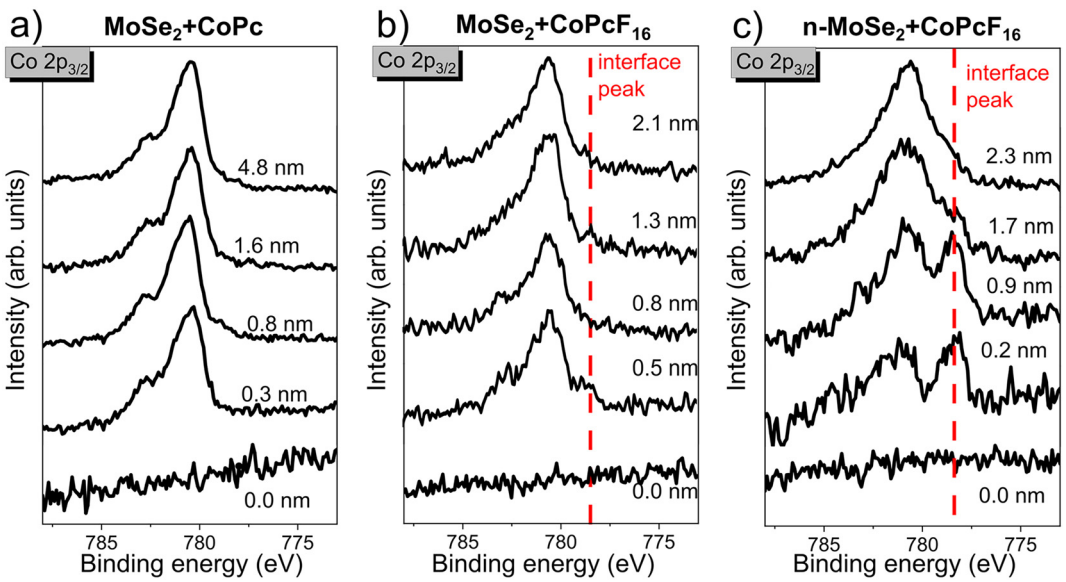


Fig. 4 Co $2p_{3/2}$ core level spectra ($h\nu$ = 1486.6 eV) of (a) CoPc/$MoSe_2$, (b) $CoPcF_{16}$/$MoSe_2$, and (c) $CoPcF_{16}$/n-$MoSe_2$ for thicknesses ranging from (sub-)monolayer to several multilayers. The additional interface peak for $CoPcF_{16}$/n-$MoSe_2$ indicates a charge transfer to the Co ion of $CoPcF_{16}$.

layers. The peak shape is almost independent of the thickness for CoPc/$MoSe_2$ (Fig. 4a). For the $CoPcF_{16}/MoSe_2$ interface (Fig. 4b) a secondary peak at a lower binding energy of 778 eV is detectable at low coverages. This strongly suggests an electron transfer from the substrate to the Co ion of the $CoPcF_{16}$ molecule. Such an interface peak is also visible for the $CoPcF_{16}$/n-$MoSe_2$ interface but with distinctly higher intensity. Based on the relative intensity of the interface peak compared to the other peak part, it can be roughly estimated that at least 50% of the molecules interact strongly at the interface. This supports the results in Fig. 3, from which a stronger interaction for the n-$MoSe_2$ substrate was supposed, and confirms occurrence of an interfacial charge transfer involving the Co ion, at least for a part of the molecules directly at the interface.

We note that final state screening effects cannot be neglected in the interpretation of photoemission data. Polarization screening would shift the binding energies to lower values by some tenths of eV in the vicinity to substrates with high dielectric constants like metals (*e.g.* ref. 53). The most efficient screening mechanism is charge transfer screening, where a distinct charge transfer to the photohole occurs in the time scale of photoemission. For more reactive interfaces, it was proposed that additional lines in photoemission at distinctly lower binding energy (>1 eV) could be not only attributed to ground state charge transfer, but also to charge transfer screening. Examples are Co 2p spectra of cobalt porphyrins and C 1s spectra of NTCDA (1,4,5,8-naphthalene-tetracarboxylic acid dianhydride) on Ag(111).[54,55] Since the reactivity is similar for all three substrates in our case, the occurrence of final state screening effects for $CoPcF_{16}$/n-$MoSe_2$ in Co 2p spectra seems to be rather unlikely. We therefore interpret the interface peak at low binding energy in the Co 2p spectra of Fig. 2b and c as ground-state charge transfer, in agreement with numerous other studies of cobalt phthalocyanines or porphyrins on many substrates including metals, oxides, graphene and WSe_2.[23,25,56–59] In the case of $CoPcF_{16}/WSe_2$, the occurrence of the interface peak in Co 2p spectra was accompanied by a distinct band bending in the substrate (0.5 eV).[58] For many CoPc and/or $CoPcF_{16}$ interfaces, the open shell character of the Co^{2+} ion ($3d^7$), associated with a half-filled $3d_{z^2}$ orbital, leads to enhanced reactivity, such that the interfacial interaction is governed by a local interaction between the Co $3d_{z^2}$ orbital and states of the metal substrate.[22,23,25,58]

At the substrate site, no interface peaks could be detected, even in the most surface sensitive Se 3d spectra (Fig. S6). This may indicate that no localized bonds between Co and the topmost Se atoms are formed. Alternatively, the intensity of possible interface peaks is below the detection limit due to very few (interacting) Co atoms in $CoPcF_{16}$.

3.3. Involvement of the macrocycle of the TMPcs in the interface interaction and interface energetics

While interactions of the macrocycle can involve carbon or nitrogen atoms, here we exemplarily discuss only molecule-related C 1s core level spectra (Fig. 5). Corresponding N 1s spectra can be found in the SI (Fig. S5). C 1s spectra of phthalocyanines can be well described by one component for carbons bound to carbon and hydrogen atoms (CC, blue curves in Fig. 5) and one component for pyrrolic carbon (CN, magenta). In the case of fluorinated components, an additional component at higher binding energy must be introduced for carbon bound to fluorine atoms (CF, green). All components are accompanied by shake-up satellite features; a single satellite peak, arising from $\pi \rightarrow \pi^*$ transitions, is sufficient to describe the spectra.[26,60,61]

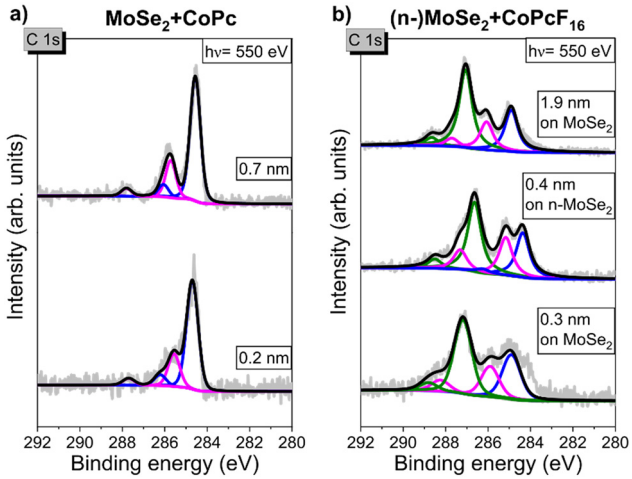


Fig. 5 Molecule related C 1s core level spectra. (a) CoPc/$MoSe_2$, (b) $CoPcF_{16}$/(n-)$MoSe_2$. Since the spectral shape is very similar for all thicknesses, the spectra do not hint to strong interactions due to chemisorption involving the carbon atoms of the macrocycle of the molecules.

The C 1s spectra in Fig. 5 can be essentially described by the same fitting model, independent of the film thickness. The detailed fitting parameters are summarized in Table S1 (SI), the fitting parameters for the N 1s spectra are depicted in Table S2 (SI). We note that the aromatic carbon component CC is in superposition with carbon from minor traces of contamination, resulting in an apparently higher intensity of this component for the lowest coverages. In addition, the binding energy separation between the CC and CN component is smaller at the interface compared to the thicker films. Such an effect was visible for phthalocyanine/metal interfaces, but also for CoPc and $CoPcF_{16}$ on MoS_2 and can be ascribed to site-dependent screening effects at the interface and/or a possible redistribution of electrons within the molecule at the interface.[26,62] Most important, no additional interface component has to be introduced in the spectra for low coverages, the spectra deliver no evidence for strong interactions due to bond formation/chemisorption and localized charge transfer to specific carbon atoms.

Since the interface formation is not yet complete at coverages in the monolayer range, we extract the energy level alignment (ELA) from UPS spectra of thicknesses > 2 nm measured in the home lab (Fig. S9); the results are depicted in Fig. 6. It is clearly evident that pronounced dipoles are observed, particularly at $CoPcFe_{16}/MoSe_2$ interfaces, while the

This journal is © The Royal Society of Chemistry 2026

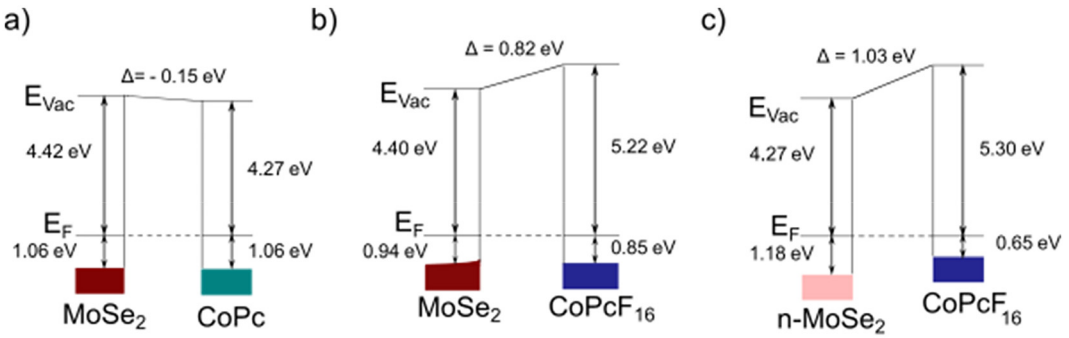


Fig. 6 Energy level alignment for coverages >2 nm: (a) CoPc/$MoSe_2$, (b) $CoPcF_{16}$/$MoSe_2$, (c) $CoPcF_{16}$/n-type $MoSe_2$.

additional n-doping of the MoSe2 leads to a further increase in the dipole. The slight shift of the top of the Γ point from 1.0 to 0.9 eV upon deposition of $CoPcF_{16}$ on nominally undoped $MoSe_2$ (Fig. 2b and e) is faintly indicated in Fig. 6b. Shifts to lower binding energies were reproduced several times in the home-lab for this interface; they are even more pronounced in the substrate-related core levels (Fig. S7 and S8). In contrast, small energetic shifts for $MoSe_2$/CoPc and n-$MoSe_2$/$CoPcF_{16}$ are not significant. Shifts to lower binding energies can be understood by an interfacial relative p-doping of the substrate, which supports the contribution of charge transfer to the interface dipoles in Fig. 6. In the case of n-$MoSe_2$, the high concentration of charge carriers at the doping level (Fig. 2c) may suppress a possible doping at this interface.

Besides charge transfer, several other effects contribute to the work function modification at interfaces (*e.g.* ref. 29 and 63), which makes a general discussion of the ELA difficult. For heptacene on Cu(110), for example, it has been shown that the push-back effect can significantly overcompensate for the dipole resulting from electron transfer.[64] It is worthwhile to compare the experimental dipoles with CoPc(F_{16})/MoS_2 from ref. 26, since the ionization potential of MoS_2 is significantly higher (~6.0 eV) than that of $MoSe_2$ (5.4 eV; *cf.* Fig. 1), whereas the reactivity of the van der Waals surfaces should not change significantly.

Clearly visible in Fig. 7, the interface dipoles Δ correlate with the differences of ionization potentials of the molecules and the TMDC substrate IP(org) − IP(TMDC). Such a behavior is typical for a Fermi level pinning regime for the respective substrate-organic combination. It is striking that the HOMO aligns with the valence band of the substrate in each case (Fig. 6, 7 and ref. 26). On the other hand, this is not the case for nominally n-doped $MoSe_2$, where the HOMO is found at a lower binding energy and consequently also the dipole is increased, the corresponding data point seems to be an outlier in Fig. 7. It seems that the HOMO in this case is pinned at the interface state observed in Fig. 2, which is filled due to the doping of the substrate. The behavior reminds to the interface between the wide gap semiconductor ZnO and the strong electron acceptor molecule F4TCNQ, an example for simultaneous ICT and FCT, where hybrid states are filled only if the ZnO substrate is doped.[40]

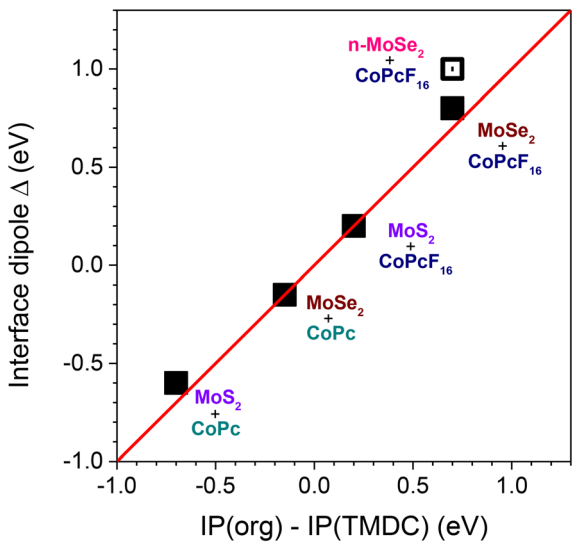


Fig. 7 Comparison of interface dipoles Δ for CoPc/MoS_2, $CoPcF_{16}$/MoS_2, CoPc/$MoSe_2$ and $CoPcF_{16}$/$MoSe_2$ as a function of differences of ionization potentials of the molecule and the substrates IP(org) − IP (TMDC). A clear correlation is visible except for the nominally n-doped $MoSe_2$.

As already briefly discussed (Fig. 2) interface states extending to the vicinity of the Fermi level were detected in the gap of $MoSe_2$ upon deposition of $CoPcF_{16}$. Since the corresponding integrated ARPES spectrum (Fig. S2) shows even a well-defined peak close to the Fermi level in the case of n-$MoSe_2$, one interpretation of this peak is the representation of the molecular HOMO. However, we rule out this hypothesis, since its distance to the C 1s core level peak (C–F component) is about 1 eV larger than C–F to HOMO (286.2 eV), as determined for bulk-like films in the home-lab. An alternative explanation is the occupation of formerly unoccupied molecular states (LUMO and even LUMO+1) at the interface, observed for several molecule/metal interfaces (*e.g.* ref. 65 and 66). We note, however, that in the case of highly ordered films the intensity maximum in ARPES energy–momentum maps (*cf.* Fig. 2f) would not be expected at Γ but around 1.5–1.7 $Å^{-1}$.[26,67–69] Further, an assignment to the (former) LUMO only seems to

be unlikely considering the strong involvement of the Co ion in the interaction at the interface. Thus, the most likely scenario in our opinion is the formation of new hybrid states at the $CoPcF_{16}/MoSe_2$ and $CoPcF_{16}$/n-$MoSe_2$ interfaces. Their intensity might be more pronounced for $CoPcF_{16}$/n-$MoSe_2$ due to the large number of available electrons in the gap of n-doped $MoSe_2$.

The interfacial charge transfer also affects the optical properties of the adsorbed $CoPcF_{16}$ molecules. In Fig. 8a we show the photoluminescence (PL) spectra taken from $CoPcF_{16}/MoSe_2$ and $CoPcF_{16}$/n-$MoSe_2$ using a home-built optical microscope (Fig. S10). To ensure comparability, all measurements are performed with identical laser excitation power and spectra integration time. To obtain an overview of the sample, 64 spectra are taken at different sample positions. The reproducibility of the spectral intensity is calculated from the deviations of the 64 spectra taken for each sample and is shown in Fig. 8a as grey ($CoPcF_{16}$/Si), red ($CoPcF_{16}/MoSe_2$), and blue ($CoPcF_{16}$/n-$MoSe_2$) shadows.

Three phenomena are observed in Fig. 8a: (1) The spectral profile is mostly identical for all three substrates. This indicates that the luminescence observed stems from the adsorbed $CoPcF_{16}$. (2) The spectral spreading for $CoPcF_{16}/MoSe_2$, and $CoPcF_{16}$/n-$MoSe_2$ is larger compared to $CoPcF_{16}$/Si, which may indicate heterogeneous interactions between the molecules and n-$MoSe_2$ and $MoSe_2$. (3) The PL spectral profiles of

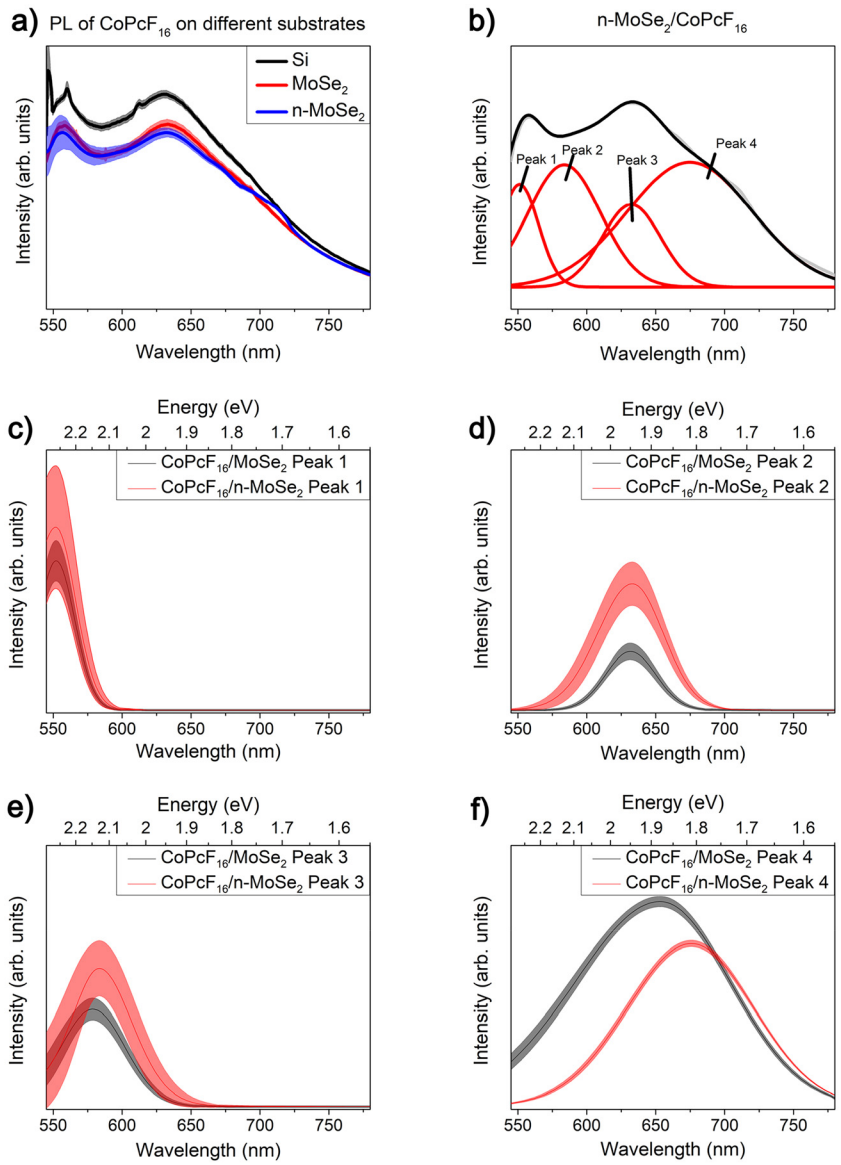


Fig. 8 Photoluminescence spectra and fitted peaks (Gaussian function) for $CoPcF_{16}$ on various substrates: (a) comparison of doped and nominally undoped $MoSe_2$ and Si substrates. (b) Representative peak fitting for a $CoPcF_{16}/MoSe_2$ PL spectrum. (c–f) Comparison of the four subpeaks. The red and grey solid lines represent the averaged spectra obtained from 64 measurements acquired on $CoPcF_{16}$/n-$MoSe_2$ and $CoPcF_{16}/MoSe_2$, respectively. The shaded areas indicate the corresponding deviations calculated from spectra collected at different sample positions.

This journal is © The Royal Society of Chemistry 2026

$CoPcF_{16}/MoSe_2$, and $CoPcF_{16}$/n-$MoSe_2$ show slight differences not only in the overall intensity, but also in the spectral shape.

To get insight into these observations, all collected spectra were spectrally fitted as exemplified for $CoPcF_{16}$/n-$MoSe_2$ in Fig. 8b. Four subpeaks (red dash lines) are used to fit the original spectra (black solid line), and the cumulative fit is shown in grey. We note that this four-component fitting procedure is empirical and a clear assignment of individual subpeaks to specific transitions is not possible without comprehensive quantum mechanical calculations. Using TDDFT methods, a large variety of possible, mostly π–π^* transitions were identified for CoPc,[70] which consequently lead to large number of possible emission pathways. The fluorination is reported to lead to a uniform shift of the orbital energies, which both keep the mentioned transitions available, while complicating the assignment further.[71] Additional challenges in the assignment arise when a molecule is deposited onto a substrate, *i.e.* the geometry of $CoPcF_{16}$ may be influenced by the adsorption onto a substrate, which in turn may influence the emission peaks.[72] Therefore, we are limited to a qualitative discussion of spectral changes at the related interfaces $CoPcF_{16}/MoSe_2$ and $CoPcF_{16}$ on nominally doped $MoSe_2$.

We first compare the maxima of the four subpeaks for $CoPcF_{16}/MoSe_2$, and $CoPcF_{16}$/n-$MoSe_2$ samples and the results are shown in Fig. 8c and d. The deviations derived from the 64 spectra taken from $CoPcF_{16}$/n-$MoSe_2$ are shown as red shadow, and the one for $CoPcF_{16}/MoSe_2$ is shown as grey shadow. For both types of samples, subpeak one appears at 552 nm, and subpeak three appears at 632 nm. Subpeak two appears at 579 nm for $CoPcF_{16}/MoSe_2$, which slightly shifts to 582 nm for $CoPcF_{16}$/n-$MoSe_2$. Subpeak 4 shows the largest change, appearing at 650 nm for $CoPcF_{16}/MoSe_2$ and at 676 nm for $CoPcF_{16}$/n-$MoSe_2$. These changes may be the result of a change of the energy levels through the interaction of the $CoPcF_{16}$ with the different substrates. Alternatively, the primary emission pathway may differ for the two differently doped $MoSe_2$ substrates. However, comprehensive quantum mechanical calculations are required to get more insight into this. Furthermore, as shown in Table S7, the intensity ratio of subpeak 4 (calculated using the integrated peak area) to the total peak intensity is about 47% for $CoPcF_{16}$/n-$MoSe_2$, while it is 69% for $CoPcF_{16}/MoSe_2$. These changes indicate a complex interaction at molecule/substrate interface, depending on the strength of the interaction and/or the amount of charge transfer.

The changes in the PL peak position and intensity agree well with the results shown in Fig. 6. With the doping of the $MoSe_2$ substrate, the energy level alignment of the molecule with the substrate varies as compared to the one without doping. Energetic shifts of particular peaks may point to a partial occupation and/or the formation of new hybrid states at the interface accompanied by charge transfer.

4. Conclusion

In conclusion, we have shown that the formation of interface states at interfaces between $MoSe_2$ and cobalt phthalocyanines crucially depends on both the ionization potential (IP) of the molecule and the doping level of the substrate. Large interface dipoles are observed for interfaces between $CoPcF_{16}$ and $MoSe_2$, where the IP of the molecule is significantly larger than the IP of $MoSe_2$. A comparison to $CoPc(F_{16})/MoS_2$ interfaces suggests that the HOMO is pinned close to the valence band maximum, *i.e.* the highest filled state of the substrate. In the case of nominal doping, the interface dipole is further increased, which may be attributed to a pinning at newly formed hybrid states visible in the ARPES band structures. Such behavior is typical for fractional charge transfer accompanied with hybridization at interfaces. XAS and PES indicate that the central cobalt atom of $CoPcF_{16}$ is involved in this interaction, suggesting that the strength of the interaction might be tuned by the choice of the TMPc. A possible scenario is that integer and fractional charge transfer (ICT and FCT) can occur simultaneously at such interfaces, depending on the charge-carrier concentration (*i.e.* doping) of $MoSe_2$, as recently proposed for F4TCNQ/ZnO/.[40]

Author contributions

The manuscript was written through contributions of all authors. Conceptualization H. P., D. Z., M. S.; data curation, investigation C. S., E. J., P. N., T. P., S. S.; formal analysis, validation and visualization, C. S., E. J., P. N., T. P.; project administration, H. P., D. Z., A. M., T. C.; supervision H. P., D. Z., A. M., T. C.; writing – original draft C. S., E. J., T. P. and H. P.; writing – review and editing, C. S., E. J., P. N., T. P., M. M., D. Z., A. M., T. C., S. S., M. S., and H. P.; funding acquisition, H. P., D. Z., T. C. and A. M. All authors have read and agreed to the published version of the manuscript.

Conflicts of interest

There are no conflicts to declare.

Data availability

The data that support the findings have been included as part of the Supplementary information (SI). Supplementary information is available. See DOI: https://doi.org/10.1039/d6nr03377f.

Further data are available from the corresponding author upon reasonable request. The upload in an openly available repository is intended.

Acknowledgements

The authors are grateful to the KIT Light Source KARA (Karlsruhe, Germany) for the provision of beamtime. The work was supported by the German Research Council (PE 546/17-1, CH 132/35-1 (project no. 511577598), ZH 279/13-1 and ME1600/21-1).

References

1 A. K. Katiyar, A. T. Hoang, D. Xu, J. Hong, B. J. Kim, S. Ji and J. H. Ahn, 2D Materials in Flexible Electronics: Recent Advances and Future Prospectives, *Chem. Rev.*, 2023, **124**(2), 318–419, DOI: 10.1021/acs.chemrev.3c00302.

2 B. Zhao, D. Y. Shen, Z. C. Zhang, P. Lu, M. Hossain, J. Li, B. Li and X. D. Duan, 2D Metallic Transition-Metal Dichalcogenides: Structures, Synthesis, Properties, and Applications, *Adv. Funct. Mater.*, 2021, (48), 31, DOI: 10.1002/adfm.202105132.

3 F. Strauss, Z. X. S. Zeng, K. Braun and M. Scheele, Toward Gigahertz Photodetection with Transition Metal Dichalcogenides, *Acc. Chem. Res.*, 2024, **57**(10), 1488–1499, DOI: 10.1021/acs.accounts.4c00088.

4 W. U. Jeong, J. B. Ahn, T. J. Jeong, Y. Ryu and S. Kim, Composition-tunable valley polarization in monolayer Mo1-xWxS2 alloys, *Curr. Appl. Phys.*, 2026, **84**, 12–18, DOI: 10.1016/j.cap.2025.12.009.

5 M. I. Alam, T. Takaoka, T. Komeda and A. Teramoto, Organic Molecule-Induced Charge Exchange in MoS2 FETs: Experimental and Theoretical Insights, *ACS Appl. Electron. Mater.*, 2026, **8**(5), 2108–2115, DOI: 10.1021/acsaelm.5c02571.

6 D. M. Soares, S. Mukherjee and G. Singh, TMDs beyond MoS2 for Electrochemical Energy Storage, *Chem. – Eur. J.*, 2020, **26**(29), 6320–6341, DOI: 10.1002/chem.202000147.

7 K. Greulich, A. Belser, S. Bölke, P. Grüninger, R. Karstens, M. S. Sättele, R. Ovsyannikov, E. Giangrisostomi, T. V. Basova, D. D. Klyamer, *et al.*, Charge Transfer from Organic Molecules to Molybdenum Disulfide: Influence of the Fluorination of Iron Phthalocyanine, *J. Phys. Chem. C*, 2020, **124**(31), 16990–16999, DOI: 10.1021/acs.jpcc.0c03862.

8 E. Juriatti, C. Späth, H. Peisert and M. Scheele, Effects of Annealing on Electrode/MoS2 Interfaces Studied by Photoelectron Spectroscopy, *ACS Appl. Electron. Mater.*, 2025, **7**(14), 6484–6490, DOI: 10.1021/acsaelm.5c00799.

9 W. Bennecke, I. G. Oliva, J. P. Bange, P. Werner, D. Schmitt, M. Merboldt, A. M. Seiler, K. Watanabe, T. Taniguchi, D. Steil, *et al.*, Hybrid Frenkel-Wannier excitons facilitate ultrafast energy transfer at a 2D-organic interface, *Nat. Phys.*, 2025, **21**(12), 1973–1980, DOI: 10.1038/s41567-025-03075-5.

10 Y. Garcia-Basabe, N. Stand, J. Arce-Molina, F. C. Vicentin, D. Steinberg and D. G. Larrude, Substrate-driven modulation of interfacial charge transfer dynamics in cobalt phthalocyanine-2D material van der Waals heterostructures, *Nanoscale*, 2026, **18**(6), 3277–3289, DOI: 10.1039/d5nr04958j.

11 S. M. Obaidulla, A. Supina, S. Kamal, Y. Khan and M. Kralj, van der Waals 2D transition metal dichalcogenide/organic hybridized heterostructures: recent breakthroughs and emerging prospects of the device, *Nanoscale Horiz.*, 2023, **9**(1), 44–92, DOI: 10.1039/d3nh00310h.

12 S. Park, T. Schultz, X. Xu, B. Wegner, A. Aljarb, A. Han, L.-J. Li, V. C. Tung, P. Amsalem and N. Koch, Demonstration of the key substrate-dependent charge transfer mechanisms between monolayer MoS2 and molecular dopants, *Commun. Phys.*, 2019, **2**(1), 109, DOI: 10.1038/s42005-019-0212-y.

13 J. Krumland and C. Cocchi, Conditions for electronic hybridization between transition-metal dichalcogenide monolayers and physisorbed carbon-conjugated molecules, *Electron. Struct.*, 2021, **3**(4), 044003, DOI: 10.1088/2516-1075/ac421f.

14 A. Champagne, O. Adeniran, J. B. Haber, F. Ricci, A. M. Alvertis, Z. F. Liu and J. B. Neaton, Tunable Electronic Energy Level Alignment and Exciton Diversity in Organic-Inorganic van der Waals Heterostructures, *ACS Nano*, 2026, **20**(8), 6572–6581, DOI: 10.1021/acsnano.5c11656.

15 M. A. Aly, D. Muth, B. Wagner, M. Koch, J. Heine and M. Gerhard, Electronic coupling and photoluminescence anisotropy in van-der-Waals-stacks of tungsten disulphide with molecular single crystals, *RSC Appl. Interfaces*, 2025, **2**(4), 1020–1030, DOI: 10.1039/d4lf00351a.

16 S. H. Amsterdam, T. J. Marks and M. C. Hersam, Leveraging Molecular Properties to Tailor Mixed-Dimensional Heterostructures beyond Energy Level Alignment, *J. Phys. Chem. Lett.*, 2021, **12**(19), 4543–4557, DOI: 10.1021/acs.jpclett.1c00799.

17 S. H. Amsterdam, T. K. Stanev, L. Q. Wang, Q. F. Zhou, S. Irgen-Gioro, S. Padgaonkar, A. A. Murthy, V. K. Sangwan, V. P. Dravid, E. A. Weiss, *et al.*, Mechanistic Investigation of Molybdenum Disulfide Defect Photoluminescence Quenching by Adsorbed Metallophthalocyanines, *J. Am. Chem. Soc.*, 2021, **143**(41), 17153–17161, DOI: 10.1021/jacs.1c07795.

18 S. Park, N. Mutz, S. A. Kovalenko, T. Schultz, D. Shin, A. Aljarb, L. J. Li, V. Tung, P. Amsalem, E. J. W. List-Kratochvil, *et al.*, Type-I Energy Level Alignment at the PTCDA-Monolayer MoS2 Interface Promotes Resonance Energy Transfer and Luminescence Enhancement, *Adv. Sci.*, 2021, **8**(12), 2100215, DOI: 10.1002/advs.202100215.

19 Y. L. Huang, Y. J. Zheng, Z. B. Song, D. Z. Chi, A. T. S. Wee and S. Y. Quek, The organic-2D transition metal dichalcogenide heterointerface, *Chem. Soc. Rev.*, 2018, **47**(9), 3241–3264, DOI: 10.1039/c8cs00159f.

20 P. Choudhury, L. Ravavarapu, R. Dekle and S. Chowdhury, Modulating Electronic and Optical Properties of Monolayer MoS2 Using Nonbonded Phthalocyanine Molecules, *J. Phys. Chem. C*, 2017, **121**(5), 2959–2967, DOI: 10.1021/acs.jpcc.6b11239.

21 S. F. Zeng, Z. W. Tang, C. S. Liu and P. Zhou, Electronics based on two-dimensional materials: Status and outlook, *Nano Res.*, 2021, **14**(6), 1752–1767, DOI: 10.1007/s12274-020-2945-z.

22 F. Ruckerl, D. Waas, B. Büchner and M. Knupfer, Particular electronic properties of F16CoPc: A decent electron acceptor material, *J. Electron Spectrosc. Relat. Phenom.*, 2017, **215**, 1–7, DOI: 10.1016/j.elspec.2016.11.013.

23 H. Peisert, J. Uihlein, F. Petraki and T. Chassé, Charge transfer between transition metal phthalocyanines and metal substrates: The role of the transition metal,

 This journal is © The Royal Society of Chemistry 2026

J. Electron Spectrosc. Relat. Phenom., 2015, **204**, 49–60, DOI: 10.1016/j.elspec.2015.01.005.

24 S. Lindner, U. Treske, M. Grobosch and M. Knupfer, Charge transfer at F16CoPc and CoPc interfaces to Au, *Appl. Phys. A: Mater. Sci. Process.*, 2011, **105**(4), 921–925, DOI: 10.1007/s00339-011-6648-x.

25 D. Balle, H. Adler, P. Grüninger, R. Karstens, R. Ovsyannikov, E. Giangrisostomi, T. Chassé and H. Peisert, Influence of the Fluorination of CoPc on the Interfacial Electronic Structure of the Coordinated Metal Ion, *J. Phys. Chem. C*, 2017, **121**(34), 18564–18574, DOI: 10.1021/acs.jpcc.7b04494.

26 P. Haizmann, E. Juriatti, M. Klein, K. Greulich, R. Ovsyannikov, E. Giangrisostomi, T. Chassé, H. Peisert and M. Scheele, Tuning the Interfacial Electronic Structure of MoS_2 by Adsorption of Cobalt Phthalocyanine Derivatives, *ACS Appl. Electron. Mater.*, 2024, **6**(4), 2467–2477, DOI: 10.1021/acsaelm.4c00094.

27 S. J. Zelewski and R. Kudrawiec, Photoacoustic and modulated reflectance studies of indirect and direct band gap in van der Waals crystals, *Sci. Rep.*, 2017, **7**, 15365, DOI: 10.1038/s41598-017-15763-1.

28 S. Y. Hu, Y. C. Lee, J. L. Shen, K. W. Chen, K. K. Tiong and Y. S. Huang, Temperature dependence of absorption edge anisotropy in 2H-MoSe2 layered semiconductors, *Solid State Commun.*, 2006, **139**(4), 176–180, DOI: 10.1016/j.ssc.2006.05.027.

29 E. Zojer, T. C. Taucher and O. T. Hofmann, The Impact of Dipolar Layers on the Electronic Properties of Organic/Inorganic Hybrid Interfaces, *Adv. Mater. Interfaces*, 2019, **6**(14), 1900581, DOI: 10.1002/admi.201900581.

30 O. T. Hofmann, P. Rinke, M. Scheffler and G. Heimel, Integer versus Fractional Charge Transfer at Metal (/Insulator)/Organic Interfaces: Cu(/NaCl)/TCNE, *ACS Nano*, 2015, **9**(5), 5391–5404, DOI: 10.1021/acsnano.5b01164.

31 S. Braun, W. R. Salaneck and M. Fahlman, Energy-Level Alignment at Organic/Metal and Organic/Organic Interfaces, *Adv. Mater.*, 2009, **21**(14–15), 1450–1472, DOI: 10.1002/adma.200802893.

32 M. Bokdam, D. Çakır and G. Brocks, Fermi level pinning by integer charge transfer at electrode-organic semiconductor interfaces, *Appl. Phys. Lett.*, 2011, **98**(11), 113303, DOI: 10.1063/1.3565963.

33 Q. Bao, O. Sandberg, D. Dagnelund, S. Sandén, S. Braun, H. Aarnio, X. Liu, W. M. Chen, R. Österbacka and M. Fahlman, Trap-Assisted Recombination via Integer Charge Transfer States in Organic Bulk Heterojunction Photovoltaics, *Adv. Funct. Mater.*, 2014, **24**(40), 6309–6316, DOI: 10.1002/adfm.201401513.

34 M. Fahlman, P. Sehati, W. Osikowicz, S. Braun, M. P. de Jong and G. Brocks, Photoelectron spectroscopy and modeling of interface properties related to organic photovoltaic cells, *J. Electron Spectrosc. Relat. Phenom.*, 2013, **190**, 33–41, DOI: 10.1016/j.elspec.2013.02.001.

35 M. Fahlman, A. Crispin, X. Crispin, S. K. M. Henze, M. P. de Jong, W. Osikowicz, C. Tengstedt and W. R. Salaneck, Electronic structure of hybrid interfaces for polymer-based electronics, *J. Phys.:Condens. Matter*, 2007, **19**(18), 20, DOI: 10.1088/0953-8984/19/18/183202.

36 O. Endo, F. Matsui, S. Kera, W. J. Chun, M. Nakamura, K. Amemiya and H. Ozaki, Observation of Hole States at Perylene/Au(110) and Au(111) Interfaces, *J. Phys. Chem. C*, 2022, **126**(37), 15971–15979, DOI: 10.1021/acs.jpcc.2c04060.

37 S. Winkler, P. Amsalem, J. Frisch, M. Oehzelt, G. Heimel and N. Koch, Probing the energy levels in hole-doped molecular semiconductors, *Mater. Horiz.*, 2015, **2**(4), 427–433.

38 M. Hollerer, D. Lüftner, P. Hurdax, T. Ules, S. Soubatch, F. S. Tautz, G. Koller, P. Puschnig, M. Sterrer and M. G. Ramsey, Charge Transfer and Orbital Level Alignment at Inorganic/Organic Interfaces: The Role of Dielectric Interlayers, *ACS Nano*, 2017, **11**(6), 6252–6260, DOI: 10.1021/acsnano.7b02449.

39 Y. Chen, X. Liu, S. Braun, Y. Wang and M. Fahlman, Image-force effects on energy level alignment at electron transport material/cathode interfaces, *J. Mater. Chem. C*, 2020, **8**(1), 173–179, DOI: 10.1039/C9TC05128G.

40 S. Erker and O. Hofmann, Fractional and Integer Charge Transfer at Semiconductor/Organic Interfaces: The Role of Hybridization and Metallicity, *J. Phys. Chem. Lett.*, 2019, **10**(4), 848–854, DOI: 10.1021/acs.jpclett.8b03857.

41 J. J. Yeh and I. Lindau, Atomic subshell photoionization cross sections and asymmetry parameters: $1 \leq Z \leq 103$, *At. Data Nucl. Data Tables*, 1985, **32**(1), 1–155, DOI: 10.1016/0092-640X(85)90016-6.

42 M. P. Seah and W. A. Dench, Quantitative electron spectroscopy of surfaces: A standard data base for electron inelastic mean free paths in solids, *Surf. Interface Anal.*, 1979, **1**(1), 2–11, DOI: 10.1002/sia.740010103.

43 M. Ashida, N. Uyeda and E. Suito, Unit Cell Metastable-Form Constants Of Various Phthalocyanines, *Bull. Chem. Soc. Jpn.*, 1966, **39**(12), 2616–2624, DOI: 10.1246/bcsj.39.2616.

44 C. A. Schneider, W. S. Rasband and K. W. Eliceiri, NIH Image to ImageJ: 25 years of image analysis, *Nat. Methods*, 2012, **9**(7), 671–675, DOI: 10.1038/nmeth.2089.

45 J. Schindelin, I. Arganda-Carreras, E. Frise, V. Kaynig, M. Longair, T. Pietzsch, S. Preibisch, C. Rueden, S. Saalfeld, B. Schmid, *et al.*, Fiji: an open-source platform for biological-image analysis, *Nat. Methods*, 2012, **9**(7), 676–682, DOI: 10.1038/nmeth.2019.

46 R. Hesse, T. Chassé, P. Streubel and R. Szargan, Error estimation in peak-shape analysis of XPS core-level spectra using UNIFIT 2003: how significant are the results of peak fits?, *Surf. Interface Anal.*, 2004, **36**(10), 1373–1383, DOI: 10.1002/sia.1925.

47 J. J. Yeh and I. Lindau, Atomic subshell photoionization cross-sections and asymmetry parameters - 1 less-than-or-equal-to z less-than-or-equal-to 103, *At. Data Nucl. Data Tables*, 1985, **32**(1), 1–155, DOI: 10.1016/0092-640x(85)90016-6.

48 K. K. Kam and B. A. Parkinson, Detailed photocurrent spectroscopy of the semiconducting group VIB transition metal

dichalcogenides, *J. Phys. Chem.*, 1982, **86**(4), 463–467, DOI: 10.1021/j100393a010.

49 M. Toader, T. G. Gopakumar, P. Shukrynau and M. Hietschold, Exploring the F16CoPc/Ag(110) Interface Using Scanning Tunneling Microscopy and Spectroscopy. 2. Adsorption-Induced Charge Transfer Effect, *J. Phys. Chem. C*, 2010, **114**(49), 21548–21554, DOI: 10.1021/jp1078295.

50 F. de Groot, Multiplet effects in X-ray spectroscopy, *Coord. Chem. Rev.*, 2005, **249**(1–2), 31–63, DOI: 10.1016/j.ccr.2004.03.018.

51 T. Kroll, R. Kraus, R. Schonfelder, V. Y. Aristov, O. V. Molodtsova, P. Hoffmann and M. Knupfer, Transition metal phthalocyanines: insight into the electronic structure from soft X-ray spectroscopy, *J. Chem. Phys.*, 2012, **137**(5), 054306, DOI: 10.1063/1.4738754.

52 T. Kroll, V. Y. Aristov, O. V. Molodtsova, Y. A. Ossipyan, D. V. Vyalikh, B. Büchner and M. Knupfer, Spin and orbital ground state of Co in cobalt phthalocyanine, *J. Phys. Chem. A*, 2009, **113**(31), 8917–8922, DOI: 10.1021/jp903001v.

53 H. Peisert, D. Kolacyak and T. Chassé, Site-Specific Charge-Transfer Screening at Organic/Metal Interfaces, *J. Phys. Chem. C*, 2009, **113**(44), 19244–19250, DOI: 10.1021/Jp9057548.

54 T. Lukasczyk, K. Flechtner, L. R. Merte, N. Jux, F. Maier, J. M. Gottfried and H. P. Steinruck, Interaction of cobalt(II) tetraarylporphyrins with a Ag(111) surface studied with photoelectron spectroscopy, *J. Phys. Chem. C*, 2007, **111**(7), 3090–3098, DOI: 10.1021/jp0652345.

55 A. Scholl, Y. Zou, T. Schmidt, R. Fink and E. Umbach, High-resolution photoemission study of different NTCDA monolayers on Ag(111): Bonding and screening influences on the line shapes, *J. Phys. Chem. B*, 2004, **108**(38), 14741–14748, DOI: 10.1021/jp049005z.

56 J. M. Gottfried, Surface chemistry of porphyrins and phthalocyanines, *Surf. Sci. Rep.*, 2015, **70**(3), 259–379, DOI: 10.1016/j.surfrep.2015.04.001.

57 M. Glaser, H. Peisert, H. Adler, U. Aygül, M. Ivanovic, P. Nagel, M. Merz, S. Schuppler and T. Chassé, Electronic structure at transition metal phthalocyanine-transition metal oxide interfaces: Cobalt phthalocyanine on epitaxial MnO films, *J. Chem. Phys.*, 2015, **142**(10), 101918, DOI: 10.1063/1.4907899.

58 F. Ruckerl, T. Klaproth, R. Schuster, B. Büchner and M. Knupfer, Surface functionalization of WSe2 by F16CoPc, *Phys. Status Solidi B*, 2017, **254**(6), 1600656, DOI: 10.1002/pssb.201600656.

59 S. Lindner, U. Treske and M. Knupfer, The complex nature of phthalocyanine/gold interfaces, *Appl. Surf. Sci.*, 2013, **267**, 62–65, DOI: 10.1016/j.apsusc.2012.06.104.

60 H. Peisert, M. Knupfer, T. Schwieger, G. G. Fuentes, D. Olligs, J. Fink and T. Schmidt, Fluorination of copper phthalocyanines: Electronic structure and interface properties, *J. Appl. Phys.*, 2003, **93**(12), 9683–9692, DOI: 10.1063/1.1577223.

61 H. Peisert, M. Knupfer and J. Fink, Electronic structure of partially fluorinated copper phthalocyanine (CuPCF4) and its interface to Au(100), *Surf. Sci.*, 2002, **515**(2–3), 491–498.

62 H. Peisert, D. Kolacyak and T. Chassé, Site-Specific Charge-Transfer Screening at Organic/Metal Interfaces, *J. Phys. Chem. C*, 2009, **113**(44), 19244–19250, DOI: 10.1021/jp9057548.

63 M. S. Sättele, A. Windischbacher, K. Greulich, L. Egger, A. Haags, H. Kirschner, R. Ovsyannikov, E. Giangrisostomi, A. Gottwald, M. Richter, *et al.*, Hexacene on Cu(110) and Ag(110): Influence of the Substrate on Molecular Orientation and Interfacial Charge Transfer, *J. Phys. Chem. C*, 2022, **126**(10), 5036–5045, DOI: 10.1021/acs.jpcc.2c00081.

64 T. G. Boné, A. Windischbacher, M. S. Sättele, K. Greulich, L. Egger, T. Jauk, F. Lackner, H. F. Bettinger, H. Peisert, T. Chassé, *et al.*, Demonstrating the Impact of the Adsorbate Orientation on the Charge Transfer at Organic–Metal Interfaces, *J. Phys. Chem. C*, 2021, **125**(17), 9129–9137, DOI: 10.1021/acs.jpcc.1c01306.

65 T. Ules, D. Luftner, E. M. Reinisch, G. Koller, P. Puschnig and M. G. Ramsey, Orbital tomography of hybridized and dispersing molecular overlayers, *Phys. Rev. B: Condens. Matter Mater. Phys.*, 2014, **90**(15), 8, DOI: 10.1103/PhysRevB.90.155430.

66 T. Boné, A. Windischbacher, L. Scheucher, F. Presel, P. Schnabl, M. S. Wagner, H. F. Bettinger, H. Peisert, T. Chasse, P. Puschnig, *et al.*, Orientation, electronic decoupling and band dispersion of heptacene on modified and nanopatterned copper surfaces, *J. Phys.:Condens. Matter*, 2023, **35**(47), 475003, DOI: 10.1088/1361-648X/acf105.

67 N. Ueno and S. Kera, Electron spectroscopy of functional organic thin films: Deep insights into valence electronic structure in relation to charge transport property, *Prog. Surf. Sci.*, 2008, **83**(10–12), 490–557, DOI: 10.1016/j.progsurf.2008.10.002.

68 M.-H. Shang, M. Nagaosa, S.-I. Nagamatsu, S. Hosoumi, S. Kera, T. Fujikawa and N. Ueno, Photoemission from valence bands of transition metal-phthalocyanines, *J. Electron Spectrosc. Relat. Phenom.*, 2011, **184**(3–6), 261–264, DOI: 10.1016/j.elspec.2010.10.006.

69 K. Schönauer, S. Weiss, V. Feyer, D. Lüftner, B. Stadtmüller, D. Schwarz, T. Sueyoshi, C. Kumpf, P. Puschnig, M. G. Ramsey, *et al.*, Charge transfer and symmetry reduction at the CuPc/Ag(110) interface studied by photoemission tomography, *Phys. Rev. B*, 2016, **94**(20), 205144, DOI: 10.1103/PhysRevB.94.205144.

70 B. Muldowney, D. Nevonen, T. Jeaydi, C. Ziegler, B. McNicholas and V. Nemykin, Identifying charge-transfer and trip-multiplet states in Co(i), Co(ii), and Co(iii) phthalocyanines using (magneto)optical spectroscopy and (TD) DFT calculations, *Dalton Trans.*, 2025, **54**(22), 8846–8869, DOI: 10.1039/d5dt00628g.

71 Q. F. Zhou, Z. F. Liu, T. J. Marks and P. Darancet, Electronic Structure of Metallophthalocyanines, MPc (M = Fe, Co, Ni, Cu, Zn, Mg) and Fluorinated MPc, *J. Phys. Chem. A*, 2021, **125**(19), 4055–4061, DOI: 10.1021/acs.jpca.0c10766.

72 S. Kundu, P. Roy, G. Fleming and N. Makri, Franck-Condon and Herzberg-Teller Signatures in Molecular Absorption and Emission Spectra, *J. Phys. Chem. B*, 2022, **126**(15), 2899–2911, DOI: 10.1021/acs.jpcb.2c00846.

 This journal is © The Royal Society of Chemistry 2026